Dentomaxillofacial Radiology (2011) 40, 133–140

http://dmfr.birjournals.org

RESEARCH

Imaging features contributing to the diagnosis of ameloblastomas and keratocystic odontogenic tumours: logistic regression analysis

Y Ariji*[,1], M Morita[1], A Katsumata[2], Y Sugita[3], M Naitoh[1], M Goto[1], M Izumi[1], Y Kise[1], K Shimozato[4], K Kurita[5], H Maeda[3] and E Ariji[1]

[1]Department of Oral and Maxillofacial Radiology, Aichi-Gakuin University School of Dentistry, Nagoya, Japan; [2]Department of Oral Radiology, Asahi University School of Dentistry, Hozumi, Japan; [3]Department of Oral Pathology, Aichi-Gakuin University School of Dentistry, Nagoya, Japan; [4]Department of Maxillofacial Surgery, Aichi-Gakuin University School of Dentistry, Nagoya, Japan; [5]Department of Oral and Maxillofacial Surgery, Aichi-Gakuin University School of Dentistry, Nagoya, Japan

Objective: The aim of this study was to clarify the characteristic imaging features that can be used to differentiate ameloblastomas from keratocystic odontogenic tumours and to examine the significant imaging features contributing to a correct diagnosis.
Methods: 60 observers (39 specialists in oral and maxillofacial radiology and 21 non-specialists) examined CT and/or panoramic images of 10 ameloblastomas and 10 keratocystic odontogenic tumours shown on a webpage and made diagnoses. Their correct answer ratios were then calculated. The imaging features of the tumours were evaluated and expressed as binary numbers or quantitative values. The imaging features that contributed to a correct diagnosis were elucidated using logistic regression analysis.
Results: The mean correct answer ratio was 61.3% $\pm$ 17.2% for the diagnosis of ameloblastomas and keratocystic odontogenic tumours. CT images produced higher correct answer ratios for diagnosis of keratocystic odontogenic tumours by specialists. The significantly different imaging features between ameloblastomas and keratocystic odontogenic tumours were the degree of bone expansion and the presence of high-density areas. The significant imaging features contributing to a correct imaging diagnosis were the number of locules, the presence of high-density areas and the inclusion of impacted teeth.
Conclusion: The presence of high-density areas is the most useful feature in the differential diagnosis of ameloblastomas and keratocystic odontogenic tumours based on comparison of the imaging features of both tumours and examination of the diagnostic contributions of these features.
Dentomaxillofacial Radiology (2011) **40,** 133–140. doi: 10.1259/dmfr/24726112

Keywords: ameloblastomas; keratocystic odontogenic tumours; logistic regression analysis; computed tomography

Introduction

Ameloblastomas and keratocystic odontogenic tumours are major odontogenic tumours of the jaw and are occasionally associated with unerupted teeth.[1] They sometimes show aggressive growth or neoplastic potential and tend to recur.[1,2] Precise pre-operative differential diagnosis between these two tumours can help surgeons to plan treatment. Ameloblastomas usually require resection and sometimes a hemimandibulectomy if they are highly infiltrative and extensive, whereas keratocystic odontogenic tumours can be treated with enucleation.[3] More conservative and effective options can also be selected, such as enucleation after decompression and marsupialization techniques, which relieve the pressure produced by the cystic fluid, allowing shrinkage of the cystic space and apposition of the bone to the cystic walls.[4]

The typical features of conventional radiograms of ameloblastomas are multilocular or unilocular radiolucent lesions with extensive thinning and expansion of the overlying cortex, and they are occasionally associated

*Correspondence to: Yoshiko Ariji, DDS PhD, Department of Oral and Maxillofacial Radiology, Aichi-Gakuin University School of Dentistry, 2-11 Suemori-dori, Chikusa-ku, Nagoya 464-8651, Japan; E-mail: yoshiko@dpc.agu.ac.jp
Received 27 October 2009; revised 2 April 2010; accepted 6 April 2010

with embedded teeth.[5] These findings are not pathognomonic for ameloblastomas and may also indicate other odontogenic tumours/cysts, such as keratocystic odontogenic tumours. Therefore, differential diagnosis by conventional radiography is difficult.[5,6]

Several investigators have attempted to differentiate between the two tumours with the use of CT and MRI.[7–10] The cystic fluids of keratocystic odontogenic tumours have a low soluble protein concentration, whereas those of ameloblastomas usually contain slightly proteinaceous fluids, occasionally associated with colloidal materials.[1] Therefore, keratocystic odontogenic tumours show lower CT density than ameloblastomas.[11] Yoshiura et al[2] reported the presence of areas of increased attenuation in the cystic cavities of keratocystic odontogenic tumours caused by desquamated keratin, which they found to be a significant diagnostic finding. The heterogeneity of CT density in keratocystic odontogenic tumours was reported to be higher than in ameloblastomas.[11] It has also been reported that the different histopathological subtypes of ameloblastoma produce different CT densities.[11] In a study of the differences between the contents of their cysts, Sumi et al[12] showed a significant difference in the apparent diffusion coefficients (ADC) of the cystic (non-enhancing) areas of the two tumours on diffusion-weighted MR images. Further studies regarding intratumoral vascularity (*i.e.* angiogenesis) in the solid portions of ameloblastomas were performed using gadolinium-enhanced MR and dynamic CT images and clarified the differences between the two tumours.[1,7,8,13]

Based on the results of these studies, we attempted to achieve more effective diagnosis using imaging modalities. We reinvestigated the conventional imaging features of ameloblastomas and keratocystic odontogenic tumours to differentiate between them. Recent years have seen an increasing demand for the teaching of CT diagnosis of odontogenic tumours to undergraduate students and residents at dental university hospitals. However, no studies have examined how the use of CT images can influence diagnosis and it has not been clarified whether experience improves the accuracy of imaging diagnosis.

In the present study, we examined the correct answer ratios for imaging diagnosis of ameloblastomas and keratocystic odontogenic tumours using panoramic and/or CT images and analysed the influence of the use of CT images and the diagnostic experience of the observer. We also examined the characteristic imaging features of both tumours and clarified the significant imaging features contributing to correct imaging diagnosis using logistic regression analysis.

Materials and methods

Patients

The patients were selected from the image database of the Department of Radiology and Diagnostic Imaging of the Aichi-Gakuin University Dental Hospital between 1998 and 2004. The image database included several types of images obtained by panoramic radiography, CT, sonography, etc. The selection criteria included patients with swelling in the mandible who demonstrated a radiolucent lesion on panoramic radiograms and those who underwent CT scans owing to a suspected odontogenic tumour or cyst of the mandible. All patients underwent surgical treatment and had a histopathological diagnosis of ameloblastoma or keratocystic odontogenic tumour. Ten patients were sequentially chosen in reverse chronological order. 10 ameloblastomas (7 males and 3 females; median age 27 years; range 10–52 years) and 10 keratocystic odontogenic tumours (7 males and 3 females; median age 33 years; range 16–59 years) were included in the subsequent analyses.

The ameloblastoma specimens were examined to identify their World Health Organization (WHO) classification patterns.[5,20] All ameloblastomas were found to belong to the solid/multicystic type according to the WHO classification.[5] Five ameloblastomas showed a follicular pattern and the remaining five showed a plexiform pattern according to the WHO classification.[20] The keratocystic odontogenic tumours were examined for the presence or absence of parakeratinization and all were shown to have parakeratotic layers.

Preparation of image patterns and imaging diagnosis via the internet

CT images parallel to the occlusal plane or the lower border of the mandible were obtained using a Hi-SpeedNX (GE-Yokogawa Medical Systems, Tokyo, Japan) and an Asterion TSX (Toshiba Medical, Tokyo, Japan) with a slice thickness of 1 mm or 2 mm. When necessary, coronal and sagittal images were reconstructed. Panoramic images were obtained using a Veraviewepocs (J. Morita Mfg Corp., Kyoto, Japan) and an AZ 3000 (Asahi Roentgen Ind. Co., Ltd., Kyoto, Japan).

We prepared two image patterns: (A) a single presentation of panoramic images and (B) multiple presentations of CT and panoramic images (Table 1). The images were arranged at random and those of each patient were only displayed once. We explained the purpose of this study and called for participation from radiologists throughout Japan. These images were placed on the website of the Japanese Society for Oral and Maxillofacial Radiology, which was password protected. 60 radiologists enrolled in this study; 39 were specialists in oral and maxillofacial radiology and the remaining 21 were non-specialists or younger oral and maxillofacial surgeons or residents. When the observers accessed this study part on the website, image pattern A or B was presented at random. The observers were then asked whether the image was an ameloblastoma or a keratocystic odontogenic tumour. They were not given any clinical information other than the images. After they had observed the images, they gave

Table 1 Preparation of image patterns

Pattern A			*Pattern B*		
Patient no.		*Presenting images*	*Patient no.*		*Presenting images*
Am	1	P+CT	Am	1	P
	2	P		2	P+CT
	3	P+CT		3	P
	4	P		4	P+CT
	5	P+CT		5	P
	6	P		6	P+CT
	7	P+CT		7	P
	8	P		8	P+CT
	9	P+CT		9	P
	10	P		10	P+CT
KCOT	1	P+CT	KCOT	1	P
	2	P		2	P+CT
	3	P+CT		3	P
	4	P		4	P+CT
	5	P+CT		5	P
	6	P		6	P+CT
	7	P+CT		7	P
	8	P		8	P+CT
	9	P+CT		9	P
	10	P		10	P+CT

Am, ameloblastoma; KCOT, keratocystic odontogenic tumours; P, panoramic radiography; P+CT, panoramic radiography and CT

a diagnosis of either ameloblastoma or keratocystic odontogenic tumour. At the end of the test, we counted how many observers could correctly answer ameloblastoma when presented with images of ameloblastoma, and how many could correctly answer non-ameloblastoma when presented with images of keratocystic odontogenic tumour. We calculated the ratio of observers who had correctly answered to all observers for each image to find the "correct answer ratio".

Imaging features

The CT and panoramic images were evaluated by three observers who are specialists in oral and maxillofacial radiology (YA, MN and MG) with regard to the following aspects. A consensus was reached after discussion when the observers disagreed. Measurements were performed by one examiner (YA), and all imaging features were expressed as binary numbers or quantitative values:

(1) Location: When the centre of the lesion was located at the first molar or its distal region, the location was defined as "1". In cases involving the second premolar or its mesial region, the location was defined as "0".

(2) Size: We measured the maximum diameter of the lesion on the slice image in which the lesion was largest.

(3) Number of locules: Based on the number of locules, multilocular lesions were defined as "1" (Figure 1a), and unilocular lesions were defined as "0".

(4) Bone expansion: The buccolingual width of the mandible was measured on the slice image in which the lesion was most expanded. The ratio of the buccolingual width on the affected side to that on the opposite side was calculated (Figure 1b).

(5) Bone resorption: When the cortical plate of the mandible was resorbed, the lesion was defined as "1" (Figure 1c). When the cortical plate was not resorbed or it was thinned, it was defined as "0".

(6) Internal density: The CT densities of the lesion were measured on a CT workstation monitor. For density measurements, the regions of interest (ROI) consisted of circular or elliptical areas representing the largest intralesional areas, not including calcification, adjacent bone or dental tissue. If the lesion included different densities, the highest density was adopted (Figure 1d).

(7) High-density areas: We examined the presence or absence of high-density areas with CT numbers ranging from 90 HU to 220 HU. The lesions with high-density areas were defined as "1" (Figure 1e), and those without were defined as "0".

(8) Tooth resorption: Resorption of the roots of adjacent teeth was evaluated. Lesions showing tooth resorption were defined as "1" (Figure 1f), and those showing no resorption were defined as "0".

(9) Impacted tooth: We evaluated whether the crown of the impacted tooth was included in the lesion. Inclusion was defined as "1" (Figure 1g), and no inclusion was defined as "0".

Imaging features contributing to imaging diagnosis

Based on the correct answers of the observers, we analysed whether the nine imaging features mentioned above contributed to a correct imaging diagnosis.

Statistical analysis

Microsoft Excel Statistics 2008 (Microsoft Corp, Redmond, WA) was used for statistical analyses. Comparison of the correct answer ratios between the presented image patterns was performed using the Mann–Whitney *U*-test. The correct answer ratios between specialists and non-specialists and between observations with and without CT images were also analysed using the Mann–Whitney *U*-test. The Mann–Whitney *U*-test was also used to compare the imaging features measured as quantitative values (including size, bone expansion and internal density) between the two groups. Fisher's exact test was used to compare the imaging features categorized by binary numbers (including location, number of locules, bone resorption, high-density area, tooth resorption and impacted tooth). In all analyses, $P < 0.05$ was taken to indicate significance.

Logistic regression analysis was performed to assess the significant imaging features contributing to a correct imaging diagnosis. Odds ratios together with 95% confidence intervals (CI) and their corresponding *P*-values were calculated for all factors from multivariate models.

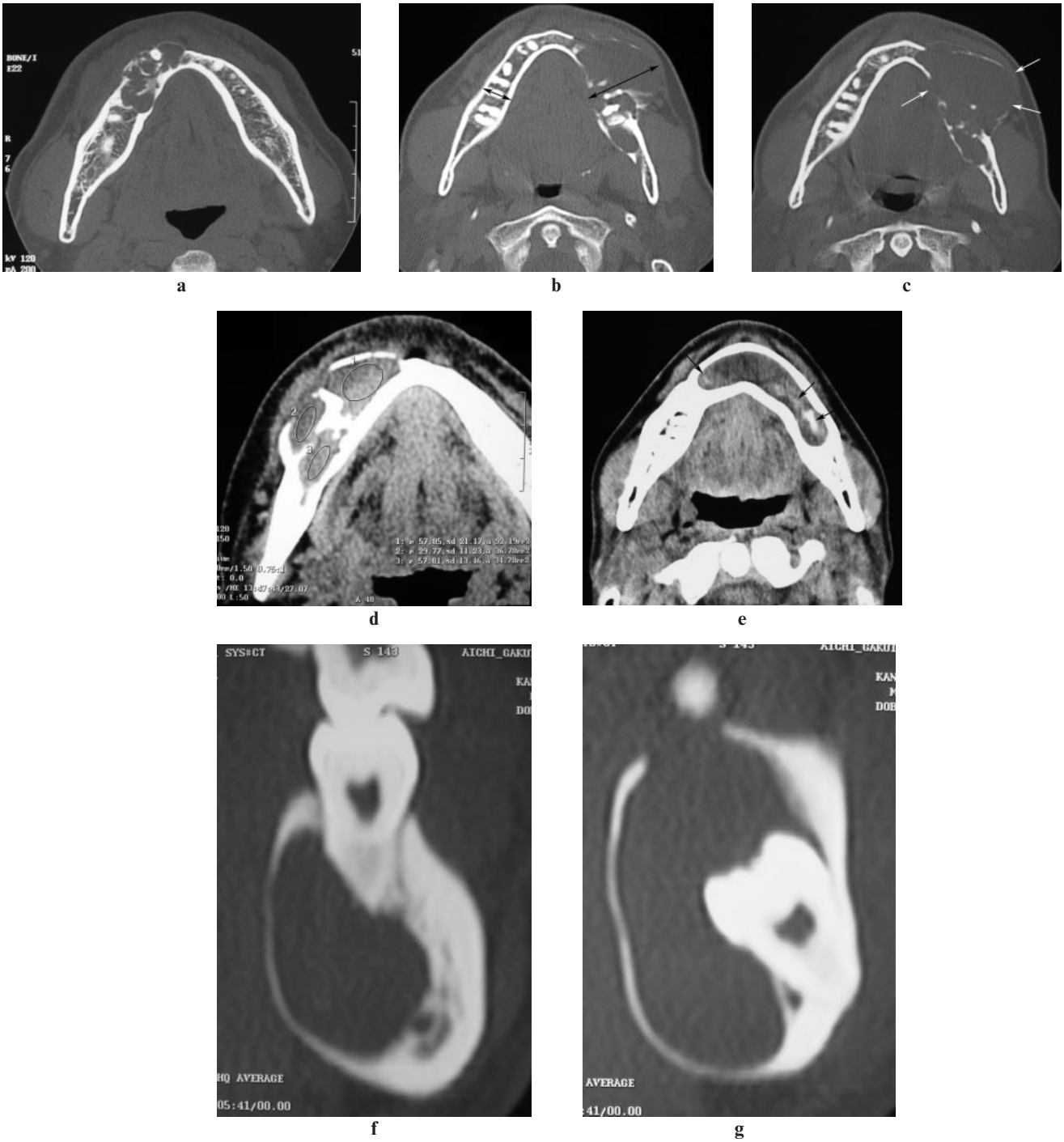

Figure 1 Imaging features. (a) Number of locules. The multilocular lesion was defined as "1". (b) Bone expansion. The buccolingual width of the mandible was measured on the CT slice image in which the lesion was most expanded. The ratio of buccolingual width on the affected side to that on the opposite side was calculated. In this case, $r = 40.4/15.7 = 2.58$. The arrows show the buccolingual width. (c) Bone resorption. The cortical plate of the mandible was resorbed, and therefore this case was defined as "1". The arrows show resorption. (d) Internal density. The CT densities of the lesion were measured. The region of interest (ROI) consisted of elliptical areas representing the largest intralesional areas not including calcification, adjacent bone or dental tissue. In this case, the CT densities of ROI 1, 2 and 3 were 57.85 HU, 29.77 HU and 57.84 HU, respectively. The highest density (57.85 HU) was adopted. (e) High-density area. The presence of high-density areas with CT numbers ranging from 90 HU to 220 HU was examined. This case was defined as "1". The arrows show the high-density areas. (f) Tooth resorption. This case had resorption of the roots of the adjacent teeth and was defined as "1". (g) Impacted tooth. The crown of the impacted tooth was included. This case was defined as "1"

Results

Imaging diagnosis on the internet

The correct answer ratios were 59.8% ± 10.7% for pattern A and 64.6% ± 15.9% for pattern B. No significant differences in the correct answer ratios were found between the two patterns ($P = 0.318$, Mann–Whitney *U*-test). The specialists accounted for 64.7% and 63.6% of the correct responses for patterns A and B, respectively. No significant differences in the ratios of the specialists to all observers were observed ($P = 0.239$, χ^2 test).

The correct answer ratios are shown in Figure 2. The mean correct answer ratios were 61.3% ± 17.2% for all observers, 63.1% ± 20.0% for the specialists and 58.3% ± 21.2% for the non-specialists. No significant difference in the correct answer ratios was found between the two observer groups ($P = 0.195$, Mann–Whitney *U*-test). In the diagnosis of ameloblastomas, no differences were observed in the correct answer ratios between the specialists and the non-specialists or between the presence and absence of CT images (specialists and non-specialists: $P = 0.940$; presence and absence of CT: $P = 0.272$, Mann–Whitney *U*-test). In the diagnosis of keratocystic odontogenic tumours by the specialists, observation using CT images led to higher correct answer ratios than without CT images ($P = 0.048$, Mann–Whitney *U*-test). In the diagnosis of keratocystic odontogenic tumours using CT images, the specialists produced higher correct answer ratios than the non-specialists ($P = 0.038$, Mann–Whitney *U*-test).

Imaging features

A summary of the imaging features of ameloblastomas and keratocystic odontogenic tumours is shown in Table 2. Significant differences between the two groups were found with regard to the degree of bone expansion and the presence of high-density areas. The mean bone expansion was 1.80 ± 0.62 in ameloblastomas and 1.36 ± 0.29 in keratocystic odontogenic tumours. Bone expansion was significantly different between the two groups ($P = 0.029$, Mann–Whitney *U*-test). High density areas were seen in six keratocystic odontogenic tumours, whereas no such areas were seen in any ameloblastoma, and the number of high-density areas was significantly different between the two groups ($P = 0.015$, Fisher's exact test). No significant differences in the other imaging features were observed between the two groups.

A comparison of the imaging features between follicular and plexiform ameloblastomas (WHO classification)[20] revealed significant differences in their size and internal density. The mean maximum diameter of the follicular ameloblastomas was 49.4 mm ± 13.9 mm and that of the plexiform ameloblastomas was 33.5 mm ± 8.8 mm. The follicular ameloblastomas were significantly larger than the plexiform ameloblastomas ($P = 0.047$, Mann–Whitney *U*-test). Their mean internal densities were 23.8 HU ± 5.3 HU and 37.7 HU ± 11.4 HU, respectively. The follicular ameloblastomas showed significantly lower density than the plexiform ameloblastomas ($P = 0.011$, Mann–Whitney *U*-test). No significant differences in the other imaging features were found between the two groups.

Imaging features contributing to imaging diagnosis

Logistic regression analysis was performed to determine the imaging features significantly contributing to correct imaging diagnosis. The results are shown in Table 3. The number of locules, the presence of high-density areas and the inclusion of impacted teeth significantly contributed to correct imaging diagnosis. Bone expansion made a slight contribution to correct diagnosis, with a *P*-value close to the significance threshold ($P = 0.0688$).

Discussion

The aim and major outcomes of this study were as follows. We targeted ameloblastomas and keratocystic odontogenic tumours, which are the most frequently occurring odontogenic tumours. The images were placed on the internet so that many radiologists were able to enrol in this study and observe the images at the same time. The images were presented in a random order with regard to ameloblastoma or keratocystic odontogenic tumour and presence or absence of CT images. We obtained results from 60 observers. Based on these data, we not only verified the features that are useful for conventional qualitative differential diagnosis between the two tumours, but also examined the significant imaging features that contribute to a correct diagnosis using logistic regression analysis. Consequently, this study provided useful information for the education of undergraduate students and residents.

Definitive diagnosis of ameloblastoma cannot be made by conventional radiography or non-enhanced CT, as it shows radiographic features similar to those of other tumours, *e.g.* keratocystic odontogenic tumour and myxoma.[1] We found that the highest correct answer ratio was obtained by specialists using CT images (63.1%).

Previous studies indicated that some conventional radiographic findings are useful for making a differential diagnosis, such as buccolingual expansion, number of locules and root resorption of the adjacent teeth.[14–16] Buccolingual bone expansion was one of the significant features identified in the present study. Ameloblastomas spread slowly by infiltration through the medullary spaces and may erode cortical bone; therefore, their radiograms often show expansion of the cortical plates.[1,15,16] The expansion of keratocystic odontogenic tumours was smaller than that of ameloblastomas, although some multilocular cases showed large expansion and some showed lingual expansion

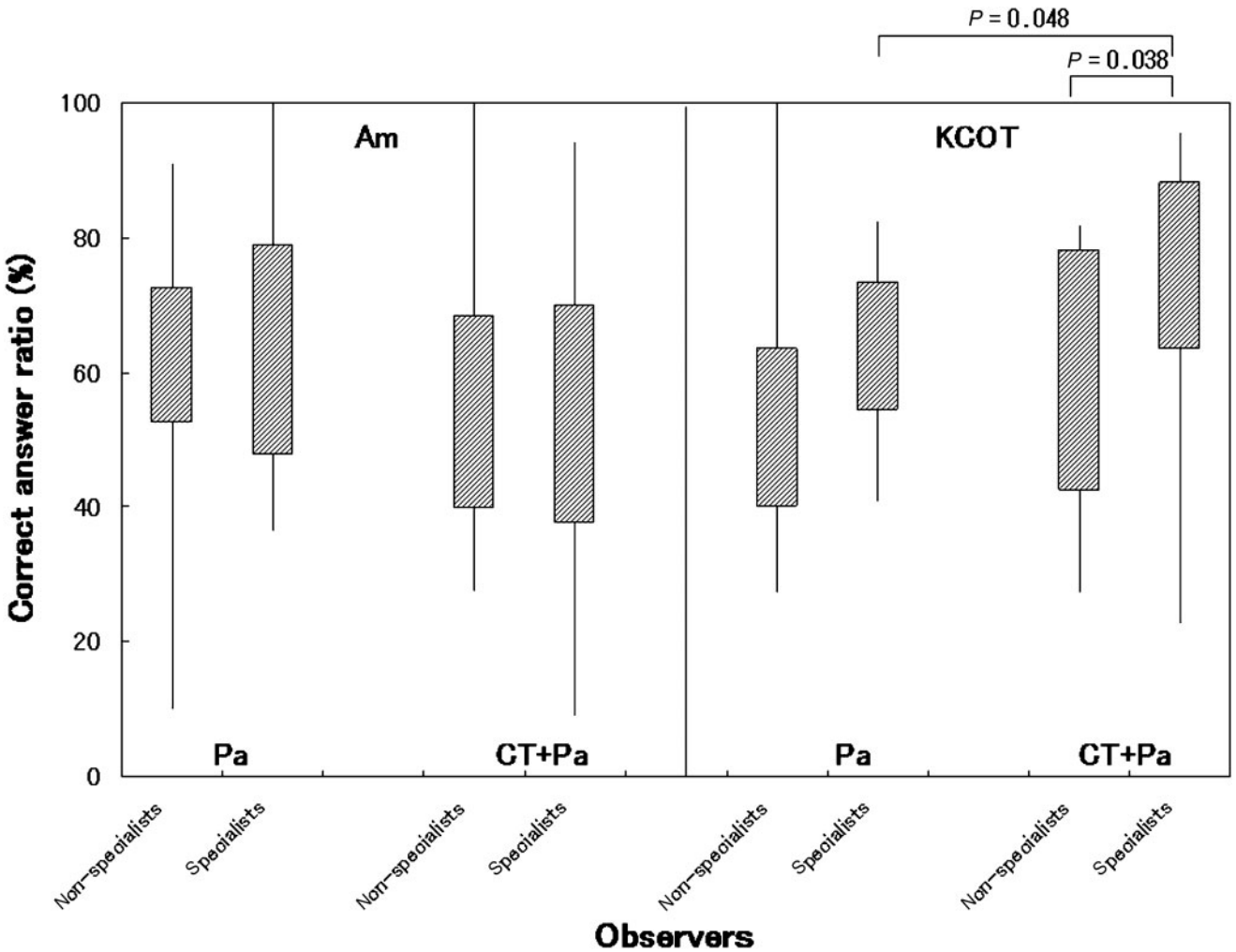

Figure 2 Correct answer ratios for all lesions, images and observers. Am, ameloblastoma; KCOT, keratocystic odontogenic tumour; Pa, panoramic images; CT+Pa, CT and panoramic images; specialists, specialists in oral and maxillofacial radiology; non-specialists, non-specialists in oral and maxillofacial radiology or younger oral and maxillofacial surgeons or residents; correct answer ratio, the ratio of the observers who had answered correctly to all observers for each image. In the diagnosis of ameloblastomas, no differences in the correct answer ratios were found between the specialists and the non-specialists or between the presence and absence of CT images (Mann–Whitney *U*-test). In the diagnosis of keratocystic odontogenic tumours by the specialists, observation using CT images led to higher correct answer ratios than that without CT images ($P = 0.048$, Mann–Whitney *U*-test). In the diagnosis of keratocystic odontogenic tumours using CT images, the specialists showed higher correct answer ratios than the non-specialists ($P = 0.038$, Mann–Whitney *U*-test)

and perforation.[14,16] The solid/multicystic type of ameloblastoma is observed as a unilocular or multilocular radiolucency with scalloped margins, whereas keratocystic odontogenic tumours may appear as small unilocular radiolucency or larger areas of radiolucency with scalloped margins.[1,15,16] In the present study, multilocular radiolucencies were only observed in three ameloblastomas, and the remaining ameloblastomas and all keratocystic odontogenic tumours were unilocular. Resorption of the roots of adjacent teeth is common in solid/multicystic ameloblastomas, but rare in keratocystic odontogenic tumours.[1,14–16] In the present study, resorption was more frequently observed in ameloblastomas than in keratocystic odontogenic tumours. Although these two features were not significant in our analysis, they may have been useful if the number of patients had been larger.

CT and MR images may be helpful for assessing not only cortical perforation and soft-tissue involvement, but also the cystic and solid contents of tumours.[1,2,6,17–19] The cystic spaces in ameloblastomas usually contain slightly proteinaceous fluids, occasionally associated with colloidal materials,[1] whereas those in keratocystic odontogenic tumours usually contain fluids with a low soluble protein concentration.[6,19] Therefore, keratocystic odontogenic tumours usually have a lower CT density than ameloblastomas.[11] In the present study, the CT density of the former was slightly lower than that of the latter, but the difference was not significant. Desquamated keratin is sometimes observed in keratocystic odontogenic tumours in long-standing or inflamed states.[1] Desquamated keratin, which shows a CT value of 100 HU or more, accumulates in a non-homogeneous pattern within the

Table 2 Summary of patients and imaging features

	Ameloblastoma		*Keratocystic odontogenic tumour*	P-*value*
Patient information				
Numbers	10		10	
Age				
Mean ± SD	28.5 ± 15.2		35.5 ± 17.9	NS
Range	10–52		16–59	
Gender				
Male	7		7	NS
Female	3		3	
Histopathology[a]	S/M-F, 5 S/M-P, 5		Parakeratinization,10	
Imaging features				
Location		(S/M-F, S/M-P)		
1, first molar or distal region	6	(3, 3)	6	NS
0, second premolar or mesial region	4	(2, 2)	4	
Size (mm)	41.5 ± 13.8	(49.4 ± 13.9, 33.5 ± 8.8)	39.3 ± 11.7	NS
Number of locules				
1, multilocular lesion	3	(1, 2)	0	NS
0, unilocular lesion	7	(4, 3)	10	
Bone expansion	1.80 ± 0.62	(2.01 ± 0.80, 1.58 ± 0.36)	1.36 ± 0.29	$P = 0.029^{*}$
Bone resorption				
1, resorption	5	(2, 3)	5	NS
0, no resorption	5	(3, 2)	5	
Internal density (HU)	30.8 ± 11.1	(23.8 ± 5.3, 37.7 ± 11.4)	29.7 ± 13.9	NS
High density area				
1, presence	0	(0, 0)	6	$P = 0.015^{**}$
0, absence	10	(5, 5)	4	
Tooth resorption				
1, resorption	5	(3, 2)	2	NS
0, no resorption	5	(2, 3)	8	
Impacted tooth				
1, presence	4	(3, 1)	7	NS
0, absence	6	(2, 4)	3	

[a]S/M-F, solid/multicystic-follicular pattern; S/M-P, solid/multicystic-plexiform pattern; NS, not significant
*$P<0.05$, Mann-Whitney *U*-test
**$P<0.05$, Fisher's exact test

low-density fluid of the cystic cavity; this causes high CT heterogeneity.[2,11] Specialists can use this CT feature when diagnosing keratocystic odontogenic tumours, which may explain why their correct answer ratios obtained using CT images were higher than those of the non-specialists.

In a comparison of the different histopathological ameloblastoma subtypes, the tumour epithelium in the follicular pattern is arranged in the form of discrete islands and the cysts form within the epithelial islands. However, the tumour epithelium in the plexiform pattern is arranged as a network bounded by a layer of cuboidal to columnar cells and the cysts usually occur as a result of stromal degeneration.[20] In the present study, the follicular pattern tumours were significantly larger and showed lower CT density than the plexiform pattern tumours. These features may reflect histopathological differences. Unicystic ameloblastomas present significantly higher heterogeneity values than solid ameloblastomas and significantly lower values than multicystic keratocystic odontogenic tumours.[11] Keratocystic odontogenic tumours with a parakeratotic epithelium are large and multilocular compared with orthokeratotic types.[21] However, the patients enrolled in this study showed solid/multicystic ameloblastomas and keratocystic odontogenic tumours with parakeratotic layers. We were unable to examine the characteristics of the other types in the present study.

Table 3 Imaging features contributing to a correct imaging diagnosis

Predictor	*Odds ratio (95% CI)*		*P*
Location	1.07	(0.80–1.43)	0.6363
Size	1.01	(0.99–1.02)	0.2506
Number of locules	4.46	(2.63–7.58)	0.00000003**
Bone expansion	1.39	(0.98–1.98)	0.0688
Bone resorption	1.27	(0.96–1.68)	0.0971
Internal density	1.00	(0.99–1.01)	0.9441
High density area	2.01	(1.47–2.74)	0.00001**
Tooth resorption	0.76	(0.56–1.05)	0.0928
Impacted tooth	1.55	(1.05–2.29)	0.0267*

CI, confidence interval; ** $P < 0.01$; * $P < 0.05$

The significant imaging features contributing to a correct diagnosis according to logistic regression analysis were the number of locules, the presence of high-density areas and the inclusion of impacted teeth. The number of locules and the presence of high-density areas were also found to be characteristic features in previous studies,[14–16] and therefore observers should use these features to differentiate between these two tumours.

In conclusion, the mean correct answer ratio of the 60 observers was 61.3% ± 17.2% for the diagnosis of ameloblastomas and keratocystic odontogenic tumours. CT images increased the correct answer ratio for the diagnosis of keratocystic odontogenic tumours by specialists. The degree of bone expansion and the presence of high-density areas were significantly different between ameloblastomas and keratocystic odontogenic tumours. The significant imaging features contributing to a correct imaging diagnosis were the number of locules, the presence of high-density areas and the inclusion of impacted teeth. Based on comparison of ameloblastomas and keratocystic odontogenic tumours and examination of their diagnostic contributions, the presence of high-density areas may be the most effective feature for the differential diagnosis of these two tumours.

Acknowledgments

We thank all observers for their participation in the imaging diagnosis. We also thank the Japanese Society for Oral and Maxillofacial Radiology for allowing us to present the images on their website.

References

1. Barnes L, Eveson JW, Reichart P, Sidransky D. *Pathology and genetics of head and neck tumours.* Lyon: IARC Press, 2005.
2. Yoshiura K, Higuchi Y, Ariji Y, Shinohara M, Yuasa K, Nakayama E, et al. Increased attenuation in odontogenic keratocysts with computed tomography: a new finding. *Dentomaxillofac Radiol* 1994; **23**: 138–142.
3. Carlson ER, Marx RE. The ameloblastoma: primary, curative surgical management. *J Oral Maxillofac Surg* 2006; **64**: 484–494.
4. Maurette PE, Jorge J, de Moraes M. Conservative treatment protocol of odontogenic keratocyst: a preliminary study. *J Oral Maxillofac Surg* 2006; **64**: 379–383.
5. Weber AL. Imaging of cysts and odontogenic tumours of the jaw. Definition and classification. *Radiol Clin North Am* 1993; **31**: 101–120.
6. Kawai T, Murakami S, Kishino M, Matsuya T, Sakuda M, Fuchihata H. Diagnostic imaging in two cases of recurrent maxillary ameloblastoma: comparative evaluation of plain radiographs, CT and MR images. *Br J Oral Maxillofac Surg* 1998; **36**: 304–310.
7. Minami M, Kaneda T, Yamamoto H, Ozawa K, Itai Y, Ozawa M, et al. Ameloblastoma in the maxillomandibular region: MR imaging. *Radiology* 1992; **184**: 389–393.
8. Hayashi K, Tozaki M, Sugisaki M, Yoshida N, Fukuda K, Tanabe H. Dynamic multislice helical CT of ameloblastoma and odontogenic keratocyst: correlation between contrast enhancement and angiogenesis. *J Comput Assist Tomogr* 2002; **26**: 922–926.
9. Minami M, Kaneda T, Ozawa K, Yamamoto H, Itai Y, Ozawa M, et al. Cystic lesions of the maxillomandibular region: MR imaging distinction of odontogenic keratocysts and ameloblastomas from other cysts. *AJR Am J Roentgenol* 1996; **166**: 943–949.
10. Han MH, Chang KH, Lee CH, Na DG, Yeon KM, Han MC. Cystic expansile masses of the maxilla: differential diagnosis with CT and MR. *AJNR Am J Neuroradiol* 1995; **16**: 333–338.
11. Crusoé-Rebello I, Oliveira C, Campos PS, Azevedo RA, dos Santos JN. Assessment of computerized tomography density patterns of ameloblastomas and keratocystic odontogenic tumours. *Oral Surg Oral Med Oral Pathol Oral Radiol Endod* 2009; **108**: 604–608.
12. Sumi M, Ichikawa Y, Katayama I, Tashiro S, Nakamura T. Diffusion-weighted MR imaging of ameloblastomas and keratocystic odontogenic tumours: differentiation by apparent diffusion coefficients of cystic lesions. *AJNR Am J Neuroradiol* 2008; **29**: 1897–1901.
13. Tozaki M, Hayashi K, Fukuda K. Dynamic multislice helical CT of maxillomandibular lesions: distinction of ameloblastomas from other cystic lesions. *Radiat Med* 2001; **19**: 225–230.
14. Tanimoto K, Fujita M, Wada T, Koseki T, Fujiwara M, Uemura S. Radiographic features of odontogenic keratocyst in the mandibular ramus: for the differential diagnosis from ameloblastoma. *Dent Radiol* 1982; **21**: 237–245 (in Japanese).
15. Eversole LR, Rovin S. Differential radiographic diagnosis of lesions of the jawbones. *Radiology* 1972; **105**: 277–284.
16. McIvor J. The radiological features of ameloblastoma. *Clin Radiol* 1974; **25**: 237–242.
17. Heffez L, Mafee MF, Vaiana J. The role of magnetic resonance imaging in the diagnosis and management of ameloblastoma. *Oral Surg Oral Med Oral Pathol* 1988; **65**: 2–12.
18. Hertzanu Y, Mendelsohn DB, Cohen M. Computed tomography of mandibular ameloblastoma. *J Comput Assist Tomogr* 1984; **8**: 220–223.
19. van Rensburg LJ, Nortjé CJ, Thompson IO. Correlating imaging and histopathology of an odontogenic keratocyst in the nevoid basal cell carcinoma syndrome. *Dentomaxillofac Radiol* 1997; **26**: 195–199.
20. Kramer IRH, Pindborg JJ, Shear M. *Histological typing of odontogenic tumours* (2nd edn), Berlin: Springer Verlag, 1992.
21. Murakami S, Jikko A, Fujishita M, Fuchihata H, Kishino M, Furukawa Y, et al. Clinicopathological study of odontogenic keratocyst. *Oral Radiol* 1990; **6**: 27–32.